Endocrine
DOI 10.1007/s12020-014-0389-5

ENDOCRINE IMAGING

Graves' dermopathy and acropachy

Takafumi Taguchi · Hideki Nakajima · Yoshio Terada

Received: 6 August 2014 / Accepted: 7 August 2014

A 57-year-old woman was referred to hospital with verrucous nodules on her shins. Approximately 30 years ago, she underwent near-total thyroidectomy for hyperthyroidism and goiter diagnosed as Graves' disease. Postoperatively, she had normal thyroid function with levothyroxine for 30 years, but her pretibial nodules were enlarged. Physical examination showed huge verrucous nodules on her shins and dorsa of the foot (Fig. 1a) and exophthalmos. Foot X-ray showed lobular lesions on bilateral shins (Fig. 1b, arrowheads). Hand X-ray showed fluffy periosteal reaction of bones (Fig. 1c, arrowheads), soft tissue swelling (Fig. 1c, asterisks), and digital clubbing which are compatible with thyroid acropachy. Laboratory examinations showed thyroid-stimulating hormone receptor antibody levels of 380 IU/L (normal, <2.0 IU/L), thyroid-stimulating antibody values of 3,758 % (normal, ≤180 %), and thyroid-stimulating hormone blocking antibody values of 100 % (normal, ≤45.6 %). Histological examination of the nodules showed epidermal acanthosis and mucinous degeneration. She was diagnosed with pretibial myxedema associated with Graves' disease. Localized or pretibial myxedema is an infrequent extrathyroidal manifestation of Graves' disease (along with goiter, exophthalmus, thyroid acropachy, and high circulating levels of long-acting thyroid-stimulating hormone), with late onset, often occurring

T. Taguchi (✉) · Y. Terada
Department of Endocrinology, Metabolism, and Nephrology, Kochi Medical School, Kochi University, Kohasu, Oko-cho, Nankoku 783-8505, Japan
e-mail: ttagu27k@axel.ocn.ne.jp

H. Nakajima
Department of Dermatology, Kochi Medical School, Kochi University, Kohasu, Oko-cho, Nankoku 783-8505, Japan

Published online: 20 August 2014

Fig. 1 Huge verrucous nodules on her shins and dorsa of the foot (**a**). Foot X-ray showed lobular lesions on bilateral shins (**b**, *arrowheads*). Hand X-ray showed fluffy periosteal reaction of bones (**c**, *arrowheads*), soft tissue swelling (**c**, *asterisks*), and digital clubbing

after thyroidectomy or radioisotope therapy [1]. It is generally considered that thyroid dermopathy and acropachy occur with Graves' ophthalmopathy, and appear to be markers of severe ophthalmopathy [2]. Subcutaneous injections of steroids were initiated with modest improvement of myxedema after 8 months.

Disclosure No competing financial interests exist.

References

1. S. Verma, F. Rongioletti, M. Braun-Falco, T. Ruzicka, Preradial myxedema in a euthyroid male: a distinct rarity. Dermatol. Online J. **19**(4), 9 (2013)
2. V. Fatourechi, G.B. Bartley, G.Z. Eghbali-Fatourechi, C.C. Powell, D.D. Ahmed, J.A. Garrity, Graves' dermopathy and acropachy are markers of severe Graves' ophthalmopathy. Thyroid **13**(12), 1141–1144 (2003)

Endocrine
DOI 10.1007/s12020-014-0431-7

ENDOCRINE IMAGING

Natural progression of a sporadic pheochromocytoma over 15 years

Takafumi Taguchi · Toshihiro Takao · Yoshio Terada

Received: 21 August 2014 / Accepted: 15 September 2014

Keywords Pheochromocytoma · Sporadic pheochromocytoma · Natural progression

A 90-year-old woman with moderate hypertension and a left pheochromocytoma was referred to our hospital for reassessment of the pheochromocytoma. She had a history of lung cancer and no family history of endocrine tumors. She had been diagnosed with a pheochromocytoma 15 years earlier and had declined surgical treatment decidedly since then. The adrenal tumor had enlarged, as shown on serial computed tomography (CT) images, and presently measured 64 mm in diameter (Fig. 1). She was asymptomatic until recently, and received oral doxazosin mesilate and other antihypertensive drugs.

Urine catecholamine and metabolite analysis revealed the following: adrenaline 118.8 mg/day (normal 3.4–36.9 mg/day), noradrenaline 182.6 mg/day (normal 48.6–168.4 mg/day), dopamine 496.1 mg/day (normal 365.0–961.5 mg/day), vanillylmandelic acid (VMA) 18.0 mg/day (normal 1.5–4.3 mg/day), homovanillic acid (HVA) 4.4 mg/day (normal 2.1–6.3 mg/day), metanephrine 1.47 mg/day (normal 0.04–0.19 mg/day), and normetanephrine 0.63 mg/day (normal 0.09–0.33 mg/day). The urine evaluation done 15 years back showed the following: VMA 6.5 mg/day, HVA 6.6 mg/day, metanephrine 0.53 mg/day, and normetanephrine 0.58 mg/day. On serial CT (Fig. 1), a previously low-density lesion within the mass became iso-dense with niveau, indicative of cystic degeneration, beginning 2 years previously to the present. An MRI showed a low- and high-intensity left adrenal mass on T1- and T2-weighted imaging, respectively. Abnormal focal accumulation was detected in the left adrenal mass on both I-131 metaiodobenzylguanidine scintigraphy and ^{18}F-fluorodeoxyglucose positron emission tomography/CT, which was consistent with a sporadic pheochromocytoma and suggested a benign tumor based on the long history.

The natural progression of pheochromocytoma is little understood because the lesions are usually resected once diagnosed [1]. However, in elderly patients unable or unwilling to undergo surgery, longitudinal anti-hypertensive treatment is important, and a multidisciplinary approach is required [2]. Additional investigation of this condition is needed.

The cystic components and degeneration of pheochromocytoma generally reflect hemorrhagic necrosis, subsequent liquefaction, and resorption within the tumor [3]. In this particular case, the sporadic pheochromocytoma showed gradual growth with cystic degeneration over a 15-year period.

Disclosure None.

T. Taguchi (✉) · Y. Terada
Department of Endocrinology, Metabolism, and Nephrology, Kochi Medical School, Kochi University, Kohasu, Oko-cho, Nankoku 783-8505, Japan
e-mail: ttagu27k@axel.ocn.ne.jp

T. Takao
Department of Public Health, Kawasaki Medical School, 577 Matsushima, Kurashiki 701-0192, Japan

Published online: 26 September 2014

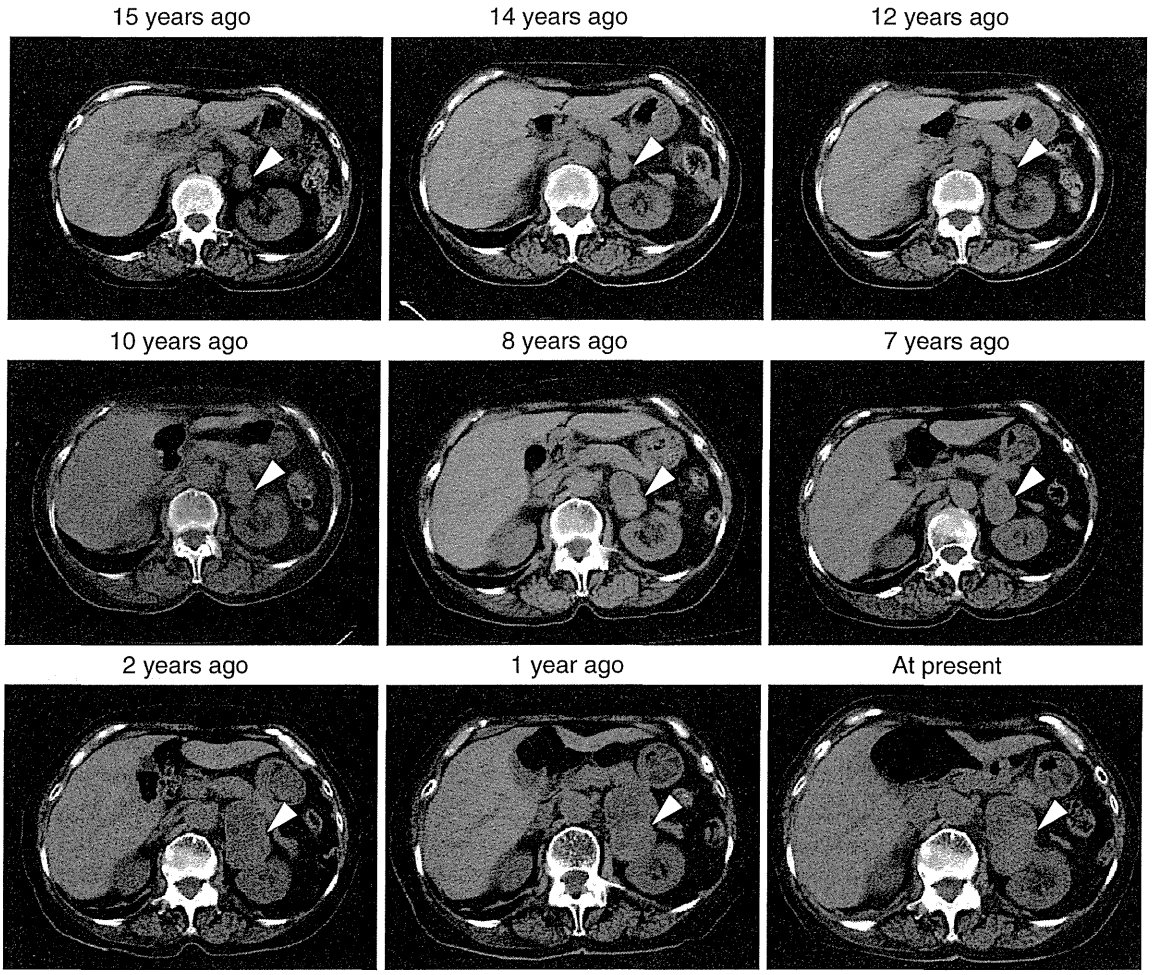

Fig. 1 Serial computed tomography performed over a 15-year period shows gradual growth of a left adrenal gland tumor (*arrowhead*), identified as a pheochromocytoma, with cystic degeneration

References

1. R. Yu, E. Ginsburg, Natural history of a sporadic pheochromocytoma. Endocr. Pract. **14**(3), 391 (2008)
2. A. Mazza, M. Armigliato, M.C. Marzola, L. Schiavon, D. Montemurro, G. Vescovo, M. Zuin, S. Chondrogiannis, R. Ravenni, G. Opocher, P.M. Colletti, D. Rubello, Anti-hypertensive treatment in pheochromocytoma and paraganglioma: current management and therapeutic features. Endocrine **45**(3), 469–478 (2014)
3. T.H. Lee, C.M. Slywotzky, M.T. Lavelle, R.A. Garcia, Cystic pheochromocytoma. Radiographics **22**(4), 935–940 (2002)

Endocrine (2014) 46:357–359
DOI 10.1007/s12020-013-0101-1

LETTER TO THE EDITOR

Lupus nephritis with positive myeloperoxidase/proteinase 3-antineutrophil cytoplasmic autoantibody that developed after 17 years of propylthiouracil therapy

Takafumi Taguchi · Shuichi Nakayama · Simpei Fujimoto · Yoshio Terada

Received: 2 July 2013 / Accepted: 23 October 2013 / Published online: 23 November 2013

Dear Editor,

Propylthiouracil (PTU) is a thiouracil-derived drug used to treat hyperthyroidism. A number of adverse effects have been reported in association with this drug, including fever, agranulocytosis, skin rash, and vasculitis. Increasing evidence has recently suggested that PTU can induce autoimmune syndromes with the production of antinuclear antibodies or antineutrophil cytoplasmic autoantibody (ANCA) in patients with Graves' disease. We herein report a patient who developed lupus nephritis with positive myeloperoxidase (MPO)/proteinase 3 (PR3)-ANCA after taking PTU for 17 years.

A 51-year-old man with a history of Graves' disease, treated with PTU at 50 mg/day for approximately 17 years, presented to another institution with persistent high fever, polyarthralgia, and foot edema and was subsequently referred to our hospital. Upon presentation, he had thrombocytopenia (platelet count, PLT: $3.8 \times 10^4/\mu L$), leukocytopenia (WBC: $2.9 \times 10^3/\mu L$ with 47 % neutrophils), microhematuria (>100 red blood cells per high-power field), proteinuria (1.01 g/day, peak value 4.26 g/day), and an elevated serum creatinine level (1.42 mg/dL, peak value 5.66 mg/dL; Fig. 1). Thyroid function tests were within the normal range. Serological examinations showed a high titer of antinuclear antibodies (1:320, speckled pattern), positive MPO-ANCA (140.0 U/mL), positive PR3-ANCA (19.5 U/mL), positive double-stranded DNA antibody (Ds-DNA IgG Ab: 19.1 IU/mL), positive single-stranded DNA antibody (Ss-DNA IgG Ab: 140.0 IU/mL), and hypocomplementemia (C_3: 41.7 mg/dL, C_4: 7.1 mg/dL, and CH_{50}: 13.9 U/mL). Renal biopsy showed mesangial proliferative glomerulonephritis, and immunofluorescence revealed positive staining for IgG, IgM, C_3, and C_{1q}. The pathological finding of a crescentic lesion indicating ANCA-associated renal vasculitis was not seen. Based on these findings, ANCA-positive lupus nephritis (WHO class II) was diagnosed. PTU treatment was discontinued, and he was effectively treated with plasmapheresis and hemodialysis combined with two pulses of cyclophosphamide and three pulses of methylprednisolone, prednisolone, and intravenous immunoglobulin therapy. After 3 months, his thrombocytopenia, proteinuria, and MPO/PR3-ANCA titer were significantly improved (Fig. 1). Potassium iodide and radioiodine therapy was administered to treat Graves' disease. At the current time point of 2-years follow-up with low-dose prednisolone, his serum creatinine level is 1.28 mg/dL with no proteinuria and microhematuria. MPO-ANCA is 12.5 IU/mL (normal range is <3.5 IU/ml) without any remarkable findings of vasculitis, and Ds-DNA/Ss-DNA IgG Ab and complement titers are within the normal range.

While the renal biopsy showed lupus nephritis, this patient had overlapping clinical and laboratory findings of lupus and vasculitis. In a previous study, ANCA was detected in 37.3 % of patients with idiopathic systemic lupus erythematosus, and patients with this condition are almost always positive for MPO-ANCA [1]. In addition, MPO-ANCA is found in a similar proportion of patients with PTU-induced lupus and patients with vasculitis; however, PR3-ANCA is detected only in patients with PTU-induced vasculitis [2]. In the present case, the regular long-term use of PTU and overlapping clinical findings of lupus and vasculitis with positive PR3-ANCA highly indicated that this patient developed an autoimmune

T. Taguchi (✉) · S. Nakayama · S. Fujimoto · Y. Terada
Department of Endocrinology, Metabolism and Nephrology, Kochi Medical School, Kochi University, Kohasu, Oko-cho, Nankoku 783-8505, Japan
e-mail: ttagu27k@axel.ocn.ne.jp

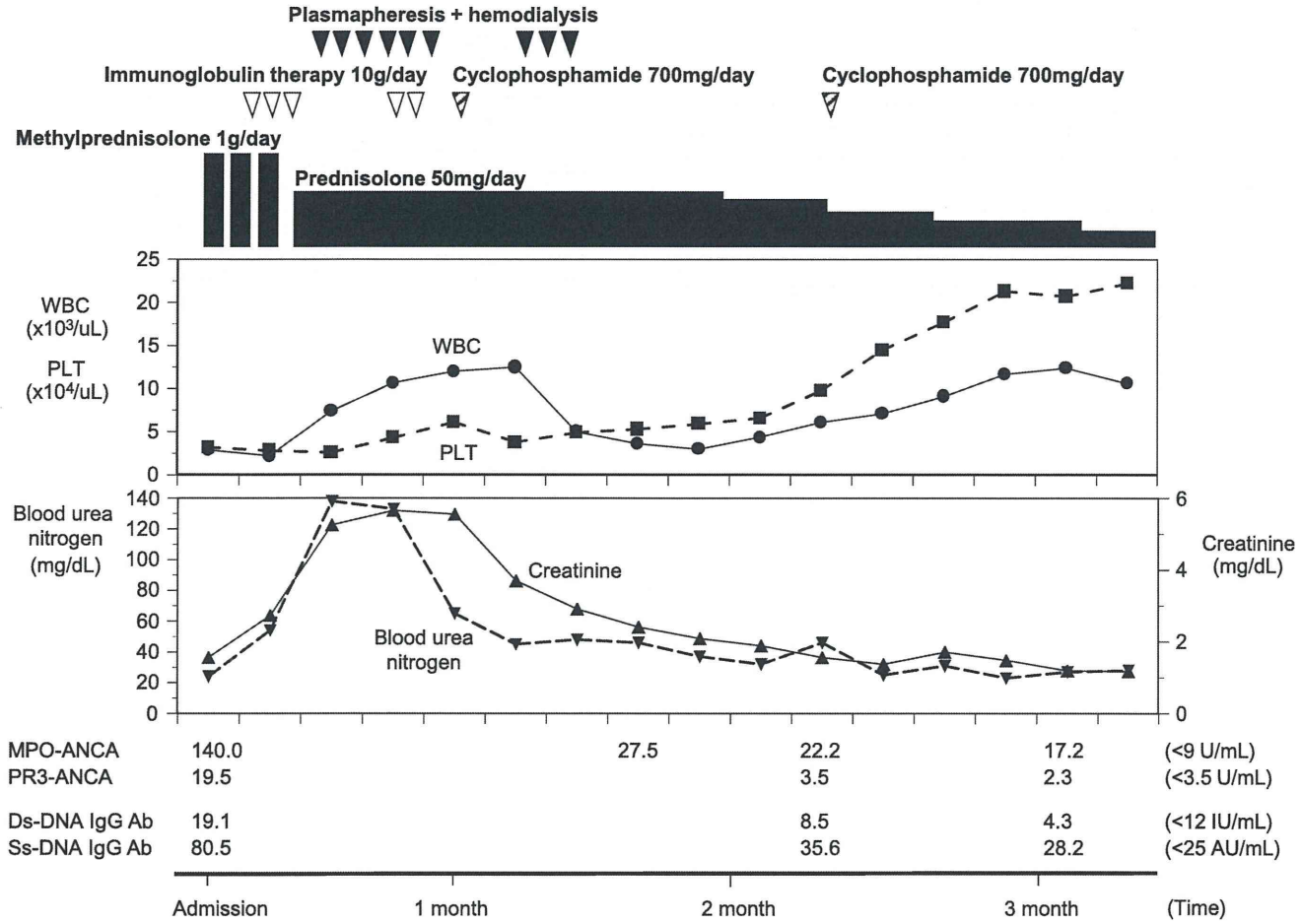

Fig. 1 Clinical course of the patient

syndrome induced by environmental factors, including drugs. However, further evidence is required as this clinical condition, termed the kaleidoscope of autoimmunity because patients with systemic lupus erythematosus often manifest features of other autoimmune diseases, is not clearly excluded [3]. Although PTU-induced lupus nephritis is rare, the reported renal biopsy findings associated with PTU are crescentic glomerulonephritis, diffuse proliferative lupus glomerulonephritis, mesangial and membranous thickening, and acute interstitial nephritis [4].

A standard treatment protocol is lacking for PTU-induced lupus nephritis with positive MPO/PR3-ANCA. We selected this intensive treatment to prevent the progression to end-stage renal disease because in addition to lupus nephritis, MPO-ANCA has the pathogenic potential for necrotizing glomerulonephritis and pulmonary capillaritis [5]. Furthermore, the patient became dialysis-dependent at an early stage with elevated blood urea nitrogen/serum creatinine levels (from 24/1.42 mg/dL to 133/5.66 mg/dL), and successfully discontinued the immunosuppressive therapy without low-dose prednisolone (Fig. 1). No obvious relapse or further elevation of MPO-ANCA occurred during the following 2 years. Further study is warranted to develop a beneficial treatment protocol.

The time of onset of PTU-induced autoimmune syndrome varies. Wu and Li [2] reported that patients with vasculitis had a longer duration of PTU than did patients with lupus (74.7 ± 29.3 vs. 32.3 ± 24.9 months, respectively). Conversely, MPO-ANCA vasculitis reportedly occurs within several weeks after the initiation of PTU [6].

It is important for physicians to be aware of these potential complications and to confirm the anti-DNA antibody titer, MPO/PR3-ANCA titer, and the presence of proteinuria and microhematuria in PTU-treated patients with Graves' disease at fixed intervals. This should be performed even when the patient has been treated with PTU for more than 15 years.

References

1. V.D. Pradhan, S.S. Badakere, L.S. Bichile, A.F. Almeida, Anti-neutrophil cytoplasmic antibodies (ANCA) in systemic lupus erythematosus: prevalence, clinical associations and correlation with other autoantibodies. J. Assoc. Physicians India **52**, 533–537 (2004)
2. R. Wu, R. Li, Propylthiouracil-induced autoimmune syndromes: 11 case report. Rheumatol. Int. **32**, 679–681 (2012)
3. M. Lorber, M.E. Gershwin, Y. Shoenfeld, The coexistence of systemic lupus erythematosus with other autoimmune diseases: the kaleidoscope of autoimmunity. Semin. Arthritis Rheum. **24**, 105–113 (1994)
4. G.V. Prasad, S. Bastacky, J.P. Johnson, Propylthiouracil-induced diffuse proliferative lupus nephritis: review of immunological complications. J. Am. Soc. Nephrol. **8**, 1205–1210 (1997)
5. X. Bosch, A. Guilabert, J. Font, Antineutrophil cytoplasmic antibodies. Lancet **368**, 404–418 (2006)
6. M. Kimura, T. Seki, H. Ozawa et al., The onset of antineutrophil cytoplasmic antibody-associated vasculitis immediately after methimazole was switched to propylthiouracil in a woman with Graves' disease who wished to become pregnant. Endocr. J. **60**, 383–388 (2013)

Endocrine (2014) 47:965–966
DOI 10.1007/s12020-014-0224-z

ENDOCRINE IMAGING

Concentric-ring sign in adrenal hemorrhage

Takafumi Taguchi · Keiji Inoue · Yoshio Terada

Received: 10 February 2014 / Accepted: 21 February 2014 / Published online: 8 March 2014

Keywords Adrenal hematoma · Idiopathic adrenal hemorrhage

A 30-year-old man with back pain and hypertension with no history of trauma or coagulopathy was referred to our hospital. A subsequent surveillance CT scan of the abdomen showed enlargement of the left adrenal gland. Weighted MRI showed an isointense mass (Fig. 1a, white arrowhead) surrounded by an area of bleeding (Fig. 1a, black arrow) on T1-weighted imaging consistent with adrenal hematoma with partial rupture on arrival. Adrenal hormone levels and all tumor markers were within normal limits. Abnormal accumulation was not detected both in F-18 fluorodeoxyglucose positron emission tomography/computed tomography and ^{131}I-metaiodobenzylguanidine scintigraphy. One month later, a unique MR appearance termed "concentric-ring sign" was seen, which appears as a mass lesion with a dark peripheral rim (Fig. 1b, black arrowhead) surrounding a bright ring (Fig. 1b, white arrowhead) on T1-weighted image. The center of the mass lesion appeared homogeneous with intensity slightly greater than muscle. Four months later, the patient's adrenal gland showed marked reduction in size, and the concentric-ring sign had disappeared. This characteristic concentric-ring sign and the dynamic size change of the adrenal gland suggest idiopathic adrenal hemorrhage without neoplastic findings.

Concentric-ring sign is usually defined as a lesion with a thin and dark peripheral rim with a bright inner ring most distinctive on T1-weighted images, which helps establish the diagnosis of chronic hematomas [1, 2]. The finding usually appears ~3 weeks after the onset of hemorrhage [1]. In the diagnosis of adrenal tumors, concentric-ring sign is an important differential finding to confirm adrenal hemorrhage or hematoma, and clinicians should be aware that repeated short-term MRI evaluations are needed.

Disclosures No competing financial interests exist.

T. Taguchi (✉) · Y. Terada
Department of Endocrinology, Metabolism and Nephrology, Kochi Medical School, Kochi University, Kohasu, Oko-cho, Nankoku 783-8505, Japan
e-mail: ttagu27k@axel.ocn.ne.jp

K. Inoue
Department of Urology, Kochi Medical School, Kochi University, Kohasu, Oko-cho, Nankoku 783-8505, Japan

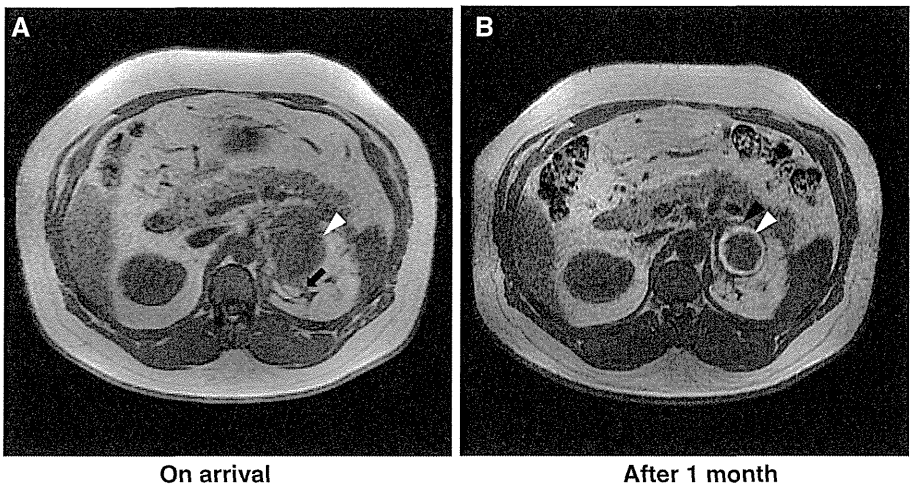

Fig. 1 MRI scans of the abdomen showing the concentric-ring sign and the change in the size of the adrenal glands. Patient's left upper abdomen with an adrenal hematoma (**a**, *white arrowhead*) with partial rupture (**a**, *black arrow*) showing isointensity on T1-weighted imaging on the patient's arrival (**a**, *white arrow head*) and concentric-ring appearance with a dark peripheral rim (**b**, *black arrowhead*) surrounding a bright ring (**b**, *white arrowhead*) on T1-weighted image after 1 month (**b**)

References

1. P.F. Hahn, S. Saini, D.D. Stark, N. Papanicolaou, J.T. Ferrucci Jr, Intraabdominal hematoma: the concentric-ring sign in MR imaging. AJR Am. J. Roentgenol. **148**(1), 115–119 (1987)
2. E.S. Siegelman, E.K. Outwater, The concentric-ring sign revisited. AJR Am. J. Roentgenol. **166**(6), 1493 (1996)

ARTHRITIS & RHEUMATOLOGY
Vol. 66, No. 3, March 2014, pp 694–706
DOI 10.1002/art.38298

Epicutaneous Application of Toll-like Receptor 7 Agonists Leads to Systemic Autoimmunity in Wild-Type Mice

A New Model of Systemic Lupus Erythematosus

Maki Yokogawa, Mikiro Takaishi, Kimiko Nakajima, Reiko Kamijima, Chisa Fujimoto, Sayo Kataoka, Yoshio Terada, and Shigetoshi Sano

Objective. **To examine whether topical treatment of wild-type mice with Toll-like receptor 7 (TLR-7) agonists leads to lupus-like autoimmunity.**

Methods. **Wild-type FVB/N, BALB/c, and C57BL/6 mice were treated with the topical TLR-7 agonist imiquimod or R848 administered to the ear 3 times weekly. During treatment, the mice were monitored for serum autoantibody and creatinine levels as well as histopathology of the kidneys, spleens, livers, hearts, and skin. Immunologic abnormalities were analyzed by immunohistochemistry, quantitative reverse transcription–polymerase chain reaction, and fluorescence-activated cell sorting. The role of plasmacytoid dendritic cells (PDCs) in the development of autoimmune disease was validated by in vivo treatment with an anti-PDC antibody. Diseased mice underwent ultraviolet B irradiation, to evaluate skin photosensitivity. The disease-causing effect of topical application of imiquimod was compared with that of systemic (intraperitoneal) administration. TLR-7– and TLR-9–deficient mice were used to validate the role of TLR-7.**

Results. **Wild-type mice of different genetic backgrounds developed systemic autoimmune disease following 4 weeks of topical treatment with imiquimod or R848, with elevated levels of autoantibodies to double-stranded DNA and multiple organ involvement, including glomerulonephritis, hepatitis, carditis, and photosensitivity. Expression of *Ifna* and *Mx1*, the interferon-α–stimulated gene, was up-regulated in the organs of imiquimod-treated mice. However, disease caused by intraperitoneal injection of imiquimod was less severe than that induced by topical application. In vivo depletion of PDCs by a specific antibody protected mice against the autoimmunity induced by topical administration of imiquimod, suggesting a role of PDCs. Furthermore, TLR-7–deficient mice, but not TLR-9–deficient mice, were protected against autoimmunity.**

Conclusion. **This protocol provides a novel model of inducible systemic lupus erythematosus in wild-type mice and underscores the skin as the primary organ that allows TLR-7 agonists to induce SLE.**

Systemic lupus erythematosus (SLE) is the prototypical human autoimmune disease and is characterized by the production of autoantibodies and the subsequent development of inflammatory disorders such as glomerulonephritis (1). Several studies have demonstrated that altered Toll-like receptor (TLR) signaling contributes to the initiation and/or exacerbation of lupus in humans and in murine models (2,3). In recent years, it has become apparent that TLR-7 and TLR-9, which sense single-stranded RNA and unmethylated DNA, respectively, contribute to the development of autoimmune diseases such as rheumatoid arthritis, SLE, and psoriasis (3,4).

TLR-7 and TLR-9 activation in dendritic cells (DCs) induces the production of inflammatory cytokines such as interleukin-6, tumor necrosis factor α, and type I interferons (IFNs) (5). In addition, autoreactive B cells, in which TLR-7/TLR-9 activation occurs in response to RNA- and DNA-containing antigens, respec-

Maki Yokogawa, MD, PhD, Mikiro Takaishi, DVM, PhD, Kimiko Nakajima, MD, PhD, Reiko Kamijima, BS, Chisa Fujimoto, BS, Sayo Kataoka, MS, Yoshio Terada, MD, PhD, Shigetoshi Sano, MD, PhD: Kochi University, Nankoku, Japan.

Address correspondence to Shigetoshi Sano, MD, PhD, Department of Dermatology, Kochi Medical School, Kochi University, Kohasu, Okocho, Nankoku, Kochi 783-8505, Japan. E-mail: sano.derma@kochi-u.ac.jp.

Submitted for publication February 21, 2013; accepted in revised form November 26, 2013.

tively, in synergy with B cell receptor, undergo proliferation, isotype switching, and plasma cell differentiation, leading to the production of autoantibodies (6,7). In the last several years, accumulating evidence has shown that the role of TLR-7 may predominate over that of TLR-9 in human SLE and in mouse models of lupus. The lupus-like phenotype in the BXSB mouse strain has been linked to the *Yaa* locus, a translocation of the telomeric end of the X chromosome, which contains *Tlr7*, to the Y chromosome (8,9). The resulting duplication of *Tlr7* appears to be responsible for the production of autoantibodies and the induction of lupus nephritis, because introduction of the TLR-7–null mutation on the BXSB background significantly reduces serum levels of autoantibodies as well as the incidence of lupus nephritis (10,11).

It was previously demonstrated that TLR-7 agonists induce much higher IFNα production by peripheral blood cells in women than in men (12). This might explain the remarkable prevalence of SLE among women, although no evidence for significant X-inactivation escape of the human TLR-7 gene was observed (12,13). The *Yaa* locus produces strikingly accelerated autoimmunity when mice with the *Yaa* mutation are bred to other mouse models of lupus such as Fcγ receptor IIB (FcγRIIB)–deficient mice (14,15). A study with TLR-7–transgenic mice revealed that an increased *Tlr7* dose alone is essential and sufficient to promote autoreactive B cells with RNA specificities and myeloid cell proliferation (16). MLR/*lpr* mice bearing the TLR-7–null mutation are protected against disease, whereas those bearing the TLR-9–null mutation exhibit accelerated disease progression, including expansion of the numbers of plasmacytoid dendritic cells (PDCs) and lymphocytes, production of anti-RNP antibodies, and increased serum titers of IFNα (3,17,18). An opposing relationship between TLR-7 and TLR-9 has emerged as a potential mechanism regulating autoimmunity, and it has been suggested that TLR-9 has a regulatory role in antagonizing TLR-7 (18).

Although several studies have used lupus-prone mice to elucidate the pathogenesis of SLE, there is no murine model of inducible lupus in wild-type (WT) mice except pristane-induced lupus (19) and mice with the graft-versus-host reaction (20). Here, we show a critical role of TLR-7 activation in lupus-like autoimmune disease in WT mice elicited by epicutaneous treatment with TLR-7 agonists. In addition, our results highlight a distinct role of skin in the induction of systemic autoimmunity by TLR-7 agonists.

MATERIALS AND METHODS

Mice and in vivo treatment. FVB/N mice were purchased from Clea, and BALB/c and C57BL/6 mice were obtained from Japan SLC. All mice were 7–9-week-old females unless otherwise indicated. TLR-7– and TLR-9–null mice were on a BALB/c background (Oriental BioService). The skin on the right ears of the mice were treated topically, 3 times weekly, with either 1.25 mg of 5% imiquimod cream (Mochida Pharmaceutical) or 100 μg of resiquimod (R848; Alexis) in 100 μl of acetone. For systemic treatment, mice received intraperitoneal injections, 3 times weekly, with 125 μg of imiquimod (Tokyo Chemical Industry) in 0.5 ml 10% DMSO. To deplete PDCs, the mice were injected intraperitoneally with 500 μg of pure anti–mouse plasmacytoid dendritic cell antigen 1 (PDCA-1) antibody (Miltenyi Biotec) every 7 days during the 4-week protocol of topical treatment with imiquimod. Rat IgG2b (Miltenyi Biotec) was used as a control. For the photosensitivity experiments, 10-week-old mice treated with topical imiquimod were irradiated by ultraviolet B (UVB) using Dermaray M-DMR-1 lamp bulbs with peak emission at 311 nm, and 24 hours later the mice were killed so that histologic changes could be observed. Photosensitivity was assessed by ear thickness, based on the histologic assessments performed before and after UVB irradiation. All of the mouse experiments were performed according to protocols approved by the Institutional Animal Care and Use Committee of Kochi Medical School.

Histopathologic assessment. Tissue sections were fixed with neutral buffered formalin and embedded in paraffin. Three-micrometer sections of skin, liver, and heart were stained with hematoxylin and eosin. For the determination of kidney histopathology, the sections were stained with periodic acid–Schiff and reviewed by a pathologist in a blinded manner. Glomerular lesions were graded semiquantitatively on a scale of 0 to 2+ for mesangioproliferation, endocapillary proliferation, mesangial matrix expansion, and segmental sclerosis (0 = <10%; 1 = 10–50%; 2 = >50% of the glomeruli examined). Global glomerular lesion scores were calculated for each mouse with at least 50 glomeruli.

Immunohistochemistry and immunofluorescence. Frozen sections of spleens were stained with anti-CD11b or anti–Gr-1 (BioLegend), followed by treatment with horseradish peroxidase (HRP)–conjugated anti-rat IgG (Dako), and were visualized using diaminobenzidine (DAB) and hematoxylin as counterstaining. For analysis of the marginal zone, frozen spleen sections were stained with antibodies to Alexa Fluor 488–conjugated anti-B220 (BioLegend) and biotinylated anti–MOMA-1 (Abcam) followed by treatment with fluorochrome-conjugated streptavidin (DyLight594; Vector). Thymus glands were stained with anti-B220 (RA3-6B2; Abcam) followed by treatment with Alexa Fluor 594–conjugated anti-rat IgG (Invitrogen).

For staining of PDCs in ear skin, deparaffinized skin specimens were incubated in 10 mmoles/liter sodium citrate for 5 minutes, using a microwave oven, and then were treated with H_2O_2 and washed with phosphate buffered saline. Slides were treated with a blocking reagent (Protein Block Serum-Free; Dako) for 1 hour at room temperature and then stained with an anti-PDC antibody (120G8.04; Dendritics), followed by treatment with HRP-conjugated anti-rat IgG (Dako), and

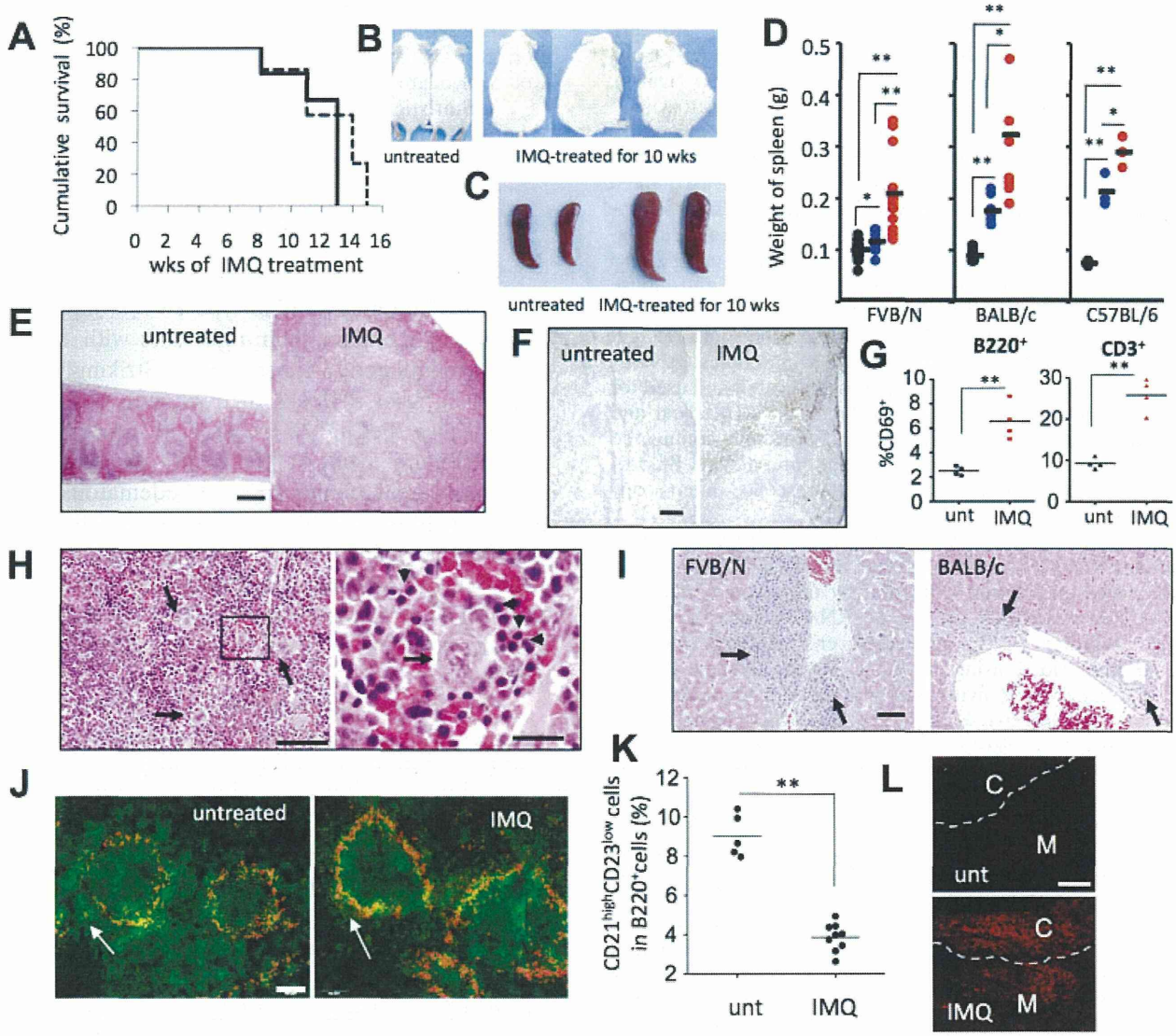

Figure 1. Fatal disease in wild-type mice following epicutaneous application of imiquimod (IMQ). **A**, Cumulative survival rate of FVB/N mice following topical application of imiquimod on ear skin 3 times weekly. Solid lines and broken lines indicate male (n = 7) and female (n = 7) mice, respectively. **B** and **C**, Swelling and edema (**B**) and marked splenomegaly (**C**) in imiquimod-treated mice at 10 weeks. **D**, Weights of spleens from FVB/N mice, BALB/c mice, and C57BL/6 mice that were untreated (unt; black circles) or treated with imiquimod for 4 weeks (blue circles) or 8 weeks (red circles). * = $P < 0.05$; ** = $P < 0.01$ by Mann-Whitney U test. **E**, Hematoxylin and eosin (H&E)–stained section of spleen from an FVB/N mouse treated with imiquimod for 10 weeks, showing increased cellularity compared with spleen from an untreated mouse. Bar = 400 μm. **F**, Increased numbers of CD11b+ cells in the spleen of imiquimod-treated BALB/c mouse compared with spleen from an untreated mouse. Images are representative of 4 independent experiments. Bar = 200 μm. **G**, Increased percentage of CD69+ cells among B lymphocytes (left) and T lymphocytes (right) in the spleens of BALB/c mice treated with imiquimod for 8 weeks compared with untreated mice. ** = $P < 0.01$ by Student's *t*-test. **H**, H&E-stained sections of spleen from an FVB/N mouse treated with imiquimod for 8 weeks, showing ectopic megakaryocytes (**arrows**) and erythroblasts (**arrowheads**). The right panel shows a higher magnification view of the boxed area in the left panel. Bars = 40 μm and 10 μm, in the left and right panels, respectively. **I**, H&E-stained section of livers from mouse treated with imiquimod for 8 weeks, showing mononuclear cell infiltrates around the portal veins of FVB/N mouse (left; **arrows**) and the bile duct of BALB/c mouse (right; **arrows**). Bar = 50 μm. **J**, Marginal zone B cell population in spleen of FVB/N mouse that was untreated (left) or treated with imiquimod for 8 weeks, as shown by staining with anti–MOMA-1 (red) and anti-B220 (green). **Arrows** indicate the marginal zone B cell areas. Bar = 100 μm. **K**, Decreased percentage of marginal zone B cells ($CD21^{high}CD23^{low}$ in gated B220+ cells) in the spleens of BALB/c mice treated with imiquimod for 8 weeks compared with untreated mice, as determined by fluorescence-activated cell sorting analysis. ** = $P < 0.01$ by Mann-Whitney U test. **L**, Anti-B220–stained sections of thymus gland from FVB/N mouse that was untreated or treated with imiquimod for 8 weeks, showing increased numbers of intrathymic B cells in diseased mouse. Broken lines indicate the boundary between the cortex (**C**) and the medulla (**M**). Bar = 100 μm. Images are representative of 4 independent experiments. In **D**, **G**, and **K**, symbols represent individual mice; horizontal lines show the mean.

visualized with DAB and counterstaining. Alternatively, PDCs were stained with anti–Siglec H antibody (440c; Abcam). Frozen skin sections were incubated with anti–Siglec H overnight, treated with HRP-conjugated anti-mouse IgG (Dako), followed by color development with DAB and hematoxylin.

Paraffin-embedded heart tissue specimens were stained with anti–Mx-1 antibody (Proteintech), followed by treatment with HRP-conjugated anti-rabbit IgG (Dako) and a color development step as described above. The direct immunofluorescence technique was performed on 6-μm acetone-fixed cryostat sections of kidneys and dorsal skin, using Alexa Fluor 488–conjugated goat anti-mouse IgG, goat anti-mouse IgM (Invitrogen), and rat anti-mouse C3 (Abcam) followed by staining with Alexa Fluor 488–conjugated rabbit anti-rat IgG (Invitrogen). For detection of antinuclear antibodies (ANAs), serum was diluted 1:80 unless otherwise indicated and used for indirect immunofluorescence on HEp-2 slides (Medical and Biological Laboratories) with Alexa Fluor 488–conjugated goat anti-mouse IgG. Sections were mounted with Fluoromount (Vector) and analyzed by fluorescence microscopy (Olympus).

Quantitative reverse transcription–polymerase chain reaction (PCR). Tissue samples were minced with scissors into small pieces on ice and disrupted by ultrasonic sonication. Total RNA was extracted using an RNA Isolation Kit (Promega) according to the manufacturer's protocol and was reverse transcribed using Moloney murine leukemia virus reverse transcriptase (Invitrogen) with random oligonucleotide hexamers (Invitrogen). PCRs were performed using Power SYBR Green PCR Master Mix (Applied Biosystems), and the amplification conditions were as follows: 50°C for 2 minutes, 90°C for 10 minutes for 1 cycle, followed by 40 cycles of 95°C for 15 seconds and 60°C for 1 minute. The following primers were used: for *Hprt*, 5′-CACAGGACTAGAACACCTGC-3′ (sense) and 5′-GCTGGTGAAAAGGACCTCT-3′ (antisense); for *Ifa*, 5′-CATTCTGCAATGACCTCCAC-3′ (sense) and 5′-TCAGGGGAAATTCCTGCAC-3′ (antisense); for *Mx1*, 5′-AAAAACCTGGATCGGAACCAA-3′ (sense) and 5′-CGGGTCAACTTCACATTCAAAG-3′ (antisense). Transcripts were analyzed using 7300 Fast System software (Applied Biosystems) and normalized to *Hprt* complementary DNA using the $\Delta\Delta C_t$ method.

Flow cytometric analysis. Splenocytes and lymph node cells were analyzed with a FACSCalibur (BD Biosciences). The following monoclonal antibodies were used: anti-CD19 (BioLegend), anti-PDC (Dendritics), anti-CD11c, anti-CD3, anti-B220, anti-CD69, anti-CD21, and anti-CD23 (all from BD Biosciences), all of which were conjugated with fluorochrome. For the staining of marginal zone B cells, splenocytes were pretreated with rat anti-mouse CD16 (BD Biosciences) on ice for 10 minutes to block FcγR before staining with anti-B220, anti-CD21, and anti-CD23 monoclonal antibodies.

Serologic analysis. The following analyses were performed using commercially available assay kits, according to the manufacturers' instructions. Serum IgG1 and IgG2a were measured by enzyme-linked immunosorbent assay (ELISA) kits (Bethyl Laboratories). Anti–double-stranded DNA (anti-dsDNA) (specific for IgG) and anti-Sm (IgG, IgA, and IgM) antibodies were detected using ELISA kits from Shibayagi and Alpha Diagnostic, respectively. Serum creatinine levels were determined using an assay kit from Cayman Chemical.

Hematology and urinalysis. Whole blood in EDTA was analyzed with a hematologic analyzer (MEK-3DN; Nihon Kohden). Urinary protein was determined using a Pyrogallol Red Molybdate protein assay kit (Wako).

Statistical analysis. Data were analyzed using Mann-Whitney 2-tailed U test and Student's *t*-test. *P* values less than 0.05 were considered significant.

RESULTS

Fatal disease in WT mice following topical treatment with imiquimod. Wild-type FVB/N mice received topical treatment on their right ears with the TLR-7 agonist imiquimod, 3 times weekly. Strikingly, they began to die after 8 weeks of treatment, and all of the treated mice died by 15 weeks, with no sexual dimorphism (Figure 1A). At 10 weeks, the torsos of the imiquimod-treated mice appeared edematous and swollen (Figure 1B). These mice also displayed marked splenomegaly (Figure 1C), which was also observed in mice with different genetic backgrounds (i.e., BALB/c and C57BL/6 mice) (Figure 1D). An equal number of male and female mice developed edema and splenomegaly.

Histologic examination of the spleens of treated mice revealed increased cellularity compared with that in untreated control mice (Figure 1E). A marked expansion in the number of myeloid cells in the spleens was observed, as indicated by staining with anti-CD11b (Figure 1F) and anti–Gr-1 (data not shown). In addition, imiquimod treatment led to increases in the numbers of both splenic B cells and splenic T cells. The mean ± SD numbers of B220+ cells from untreated mice (n = 4) and 8-week-old imiquimod-treated mice (n = 4) were $4.6 \pm 0.3 \times 10^7$/spleen and $10.1 \pm 3.4 \times 10^7$/spleen, respectively ($P < 0.01$); the mean ± SD numbers of CD3+ cells were 6.25 ± 0.65 and 15.9 ± 2.1, respectively ($P < 0.05$). Both B cells and T cells from imiquimod-treated mice also showed spontaneous activation, as indicated by an increase in the frequency of CD69 expression (Figure 1G), similar to previous observations in transgenic mice that overexpress TLR-7 (16).

Thus, topical imiquimod treatment led to the expansion and activation of both myeloid cells and lymphoid cells. Megakaryocytes and erythroblasts were observed (Figure 1H), indicating splenic extramedullary hematopoiesis. The splenic hematopoiesis might be a compensatory condition for thrombocytopenia and anemia. In fact, hematologic analysis revealed a significant reduction in the erythrocyte count, hemoglobin concentration, hematocrit, and platelet count in imiquimod-treated FVB/N mice (9%, 19%, 16%, and 64% reduc-

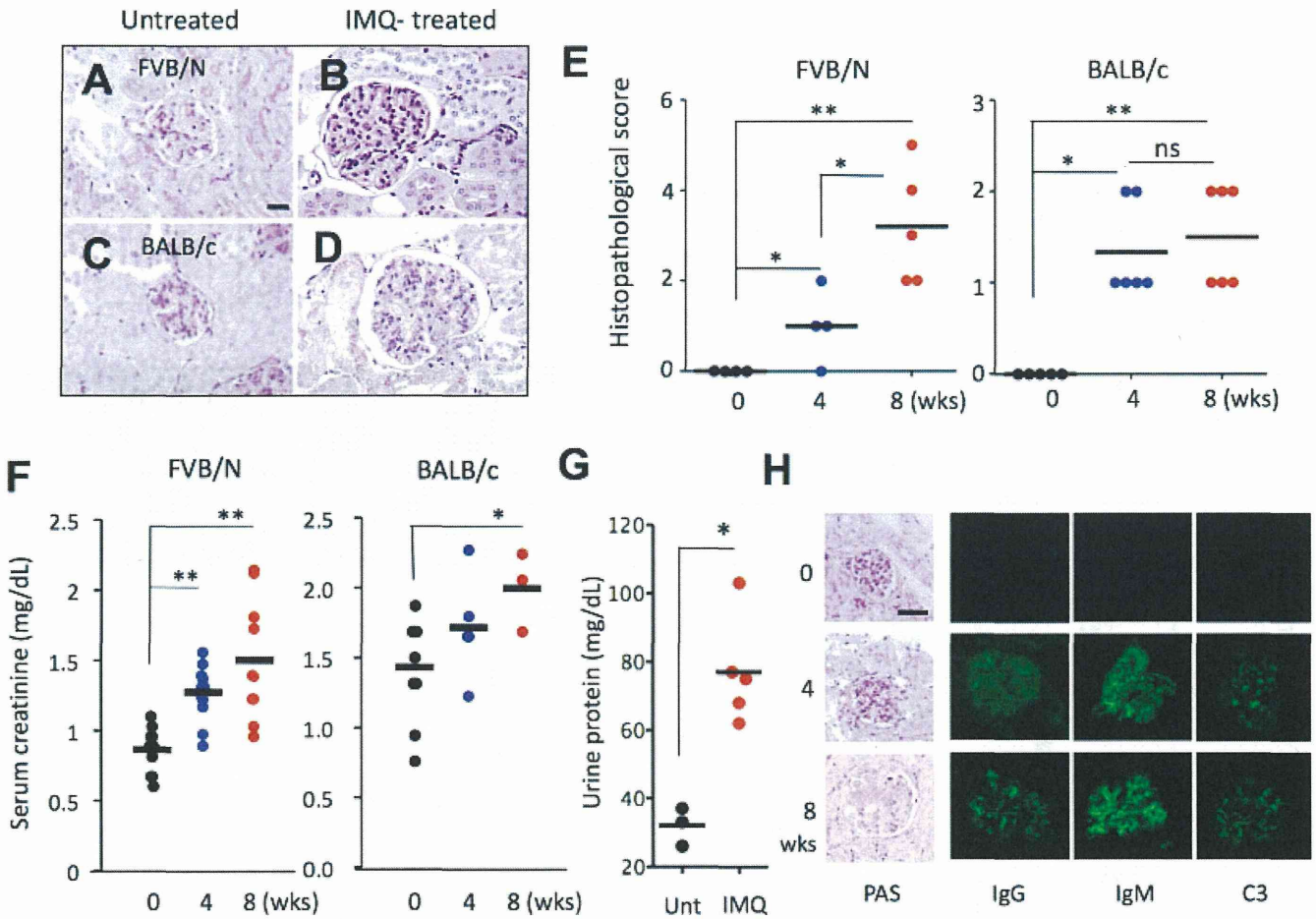

Figure 2. Glomerulonephritis in imiquimod-treated mice. **A–D**, Periodic acid–Schiff (PAS)–stained kidney sections from FVB/N mice (**A** and **B**) and BALB/c mice (**C** and **D**) that were untreated or treated with topical imiquimod for 8 weeks. Bar = 20 μm. **E**, Renal histopathologic scores in FVB/N and BALB/c mice that were untreated or treated with imiquimod for 4 weeks or 8 weeks. * = $P < 0.05$; ** = $P < 0.01$ by Mann-Whitney U test. **F**, Serum creatinine levels in FVB/N and BALB/c mice that were untreated or treated with imiquimod for 4 weeks or 8 weeks. * = $P < 0.05$; ** = $P < 0.01$ by Mann-Whitney U test. **G**, Proteinuria in BALB/c mice that were untreated or treated with imiquimod for 9 weeks. * = $P < 0.05$ by Student's *t*-test. **H**, Glomerular immune complex and C3 deposits in FVB/N mice that were untreated or treated with imiquimod for 4 weeks or 8 weeks. Renal sections were stained for PAS, IgG, IgM, and C3. Bar = 40 μm. In **E–G**, symbols represent individual mice; horizontal lines show the mean. NS = not significant (see Figure 1 for other definitions). Color figure can be viewed in the online issue, which is available at http://onlinelibrary.wiley.com/doi/10.1002/art.38298/abstract.

tions, respectively) relative to untreated mice. These hematologic abnormalities are similar to those observed in lupus-prone mice with multiple *Tlr7* transgenes (16) or in mice lacking A20 (*Tnfaip3*) (21). Livers from the diseased mice demonstrated mononuclear cell infiltrates (Figure 1I). Thus, epicutaneous application of imiquimod resulted in systemic inflammation.

Effect of topical treatment with imiquimod on B cell alteration. Spleen sections from imiquimod-treated mice demonstrated a marked reduction of the marginal zone, a characteristic rim of marginal zone B cells at the periphery of the follicles that is separated by MOMA-1–positive macrophages (Figure 1J). Notably, the numbers of MOMA-1–positive macrophages were increased by imiquimod treatment. MOMA-1–positive macrophages appear to play a role in the initial response to systemic infection (22), suggesting the effect of TLR-7 triggering. Flow cytometric analysis revealed a marked decrease in the percentage of marginal zone B cells identified as $CD21^{high}CD23^{low}$ cells (Figure 1K). The impaired development of marginal zone B cells was previously observed in BXSB-Yaa mice, $Fc\gamma RIIB^{-/-}$ Yaa mice, and transgenic mice bearing increased copy numbers of *Tlr7* (9,14,16), all of which developed systemic autoimmune disease. Also, the numbers of intrathymic B cells in diseased mice were increased (Fig-

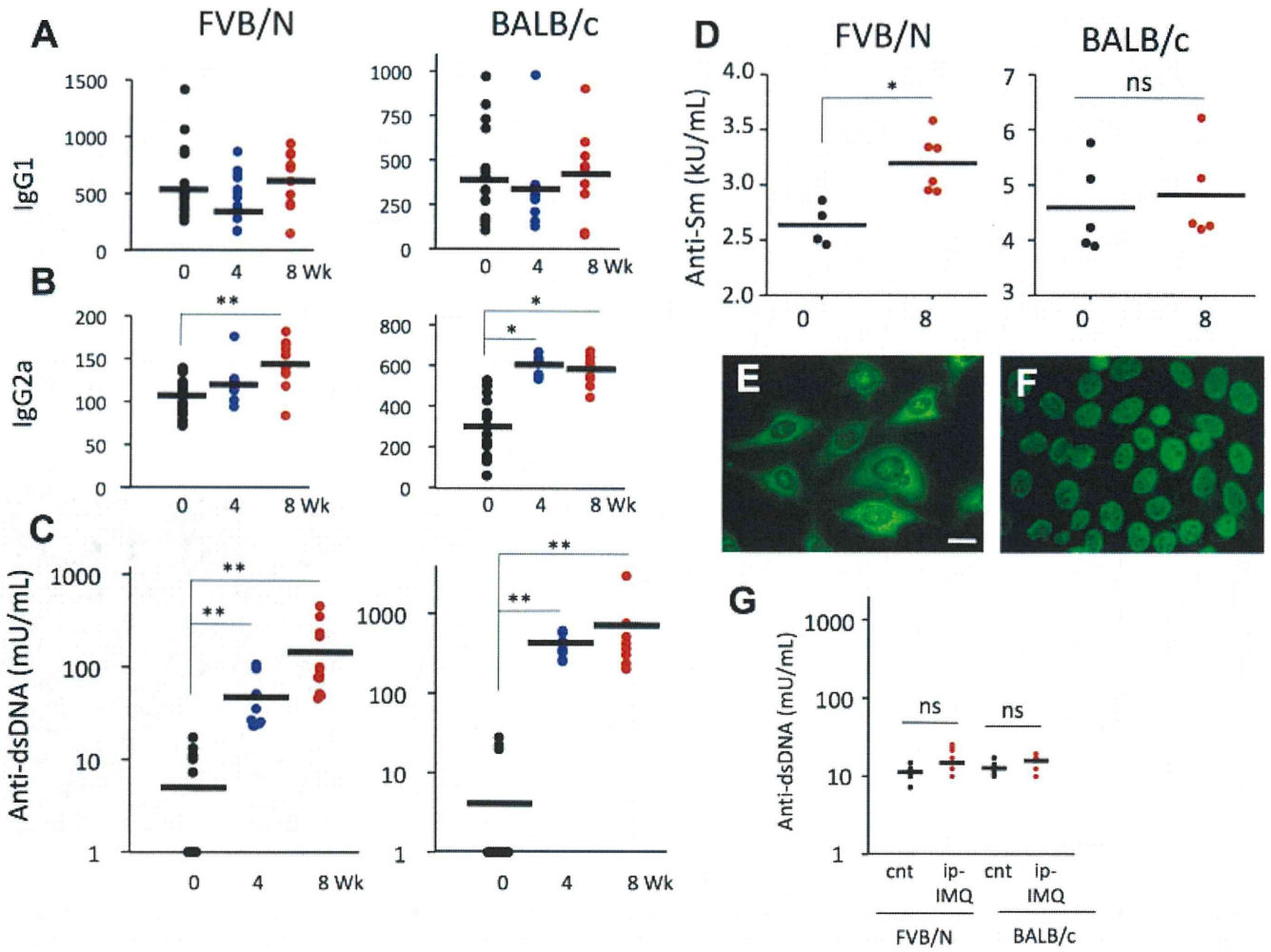

Figure 3. Induction of autoantibodies in imiquimod (IMQ)–treated mice. **A–D**, Serum IgG1 (**A**), IgG2a (**B**), anti–double-stranded DNA (anti-dsDNA) (**C**), and anti-Sm (**D**) levels in FVB/N and BALB/c mice that were untreated or treated with topical imiquimod for 4 weeks or 8 weeks, as determined by enzyme-linked immunosorbent assay. **E** and **F,** Indirect immunofluorescence analysis of sera from mouse treated with imiquimod for 8 weeks, showing anticytoplasmic antibodies and antinuclear antibodies (ANAs) with a speckled pattern in FVB/N mouse (**E**) and homogeneous/speckled ANA patterns in BALB/c mouse (**F**). Bar = 40 μm. **G**, No increase in anti-dsDNA autoantibody titers in sera from FVB/N and BALB/c mice that were untreated (control; cnt) or treated with intraperitoneal (IP) imiquimod for 4 weeks or 8 weeks. In **A–D** and **G**, symbols represent individual mice; horizontal lines show the mean. $* = P < 0.05$; $** = P < 0.01$ by Mann-Whitney U test. NS = not significant. Color figure can be viewed in the online issue, which is available at http://onlinelibrary.wiley.com/doi/10.1002/art.38298/abstract.

ure 1L), as previously observed in lupus-prone (NZB × NBW)F_1 mice (23).

Topical imiquimod–induced lupus-like glomerulonephritis in WT mice. Beginning 4 weeks after topical imiquimod treatment, histopathologic assessment of the kidneys showed enlarged hypercellular glomeruli, an increase in the mesangial matrix, and mild peritubular mononuclear cell infiltrates (Figures 2A–D). A significant increase in the renal histopathologic score was observed beginning 4 weeks after imiquimod treatment (Figure 2E). Simultaneously, elevated serum creatinine levels (Figure 2F) and increased proteinuria (Figure 2G) were observed, indicating renal dysfunction. Immunofluorescence analysis detected IgG, IgM, and C3 deposits within the glomeruli beginning 4 weeks after imiquimod treatment (Figure 2H), suggesting glomerulonephritis with immune complex deposits.

Autoantibody production induced by topical imiquimod treatment. Among diseased mice treated with imiquimod, serum IgG1 levels remained unchanged, while serum IgG2a levels were significantly elevated, beginning at week 4 (Figures 3A and B). IgG2a is the most prominent IgG subclass involved in inducing autoimmunity, while IgG1 displays the poorest pathogenicity

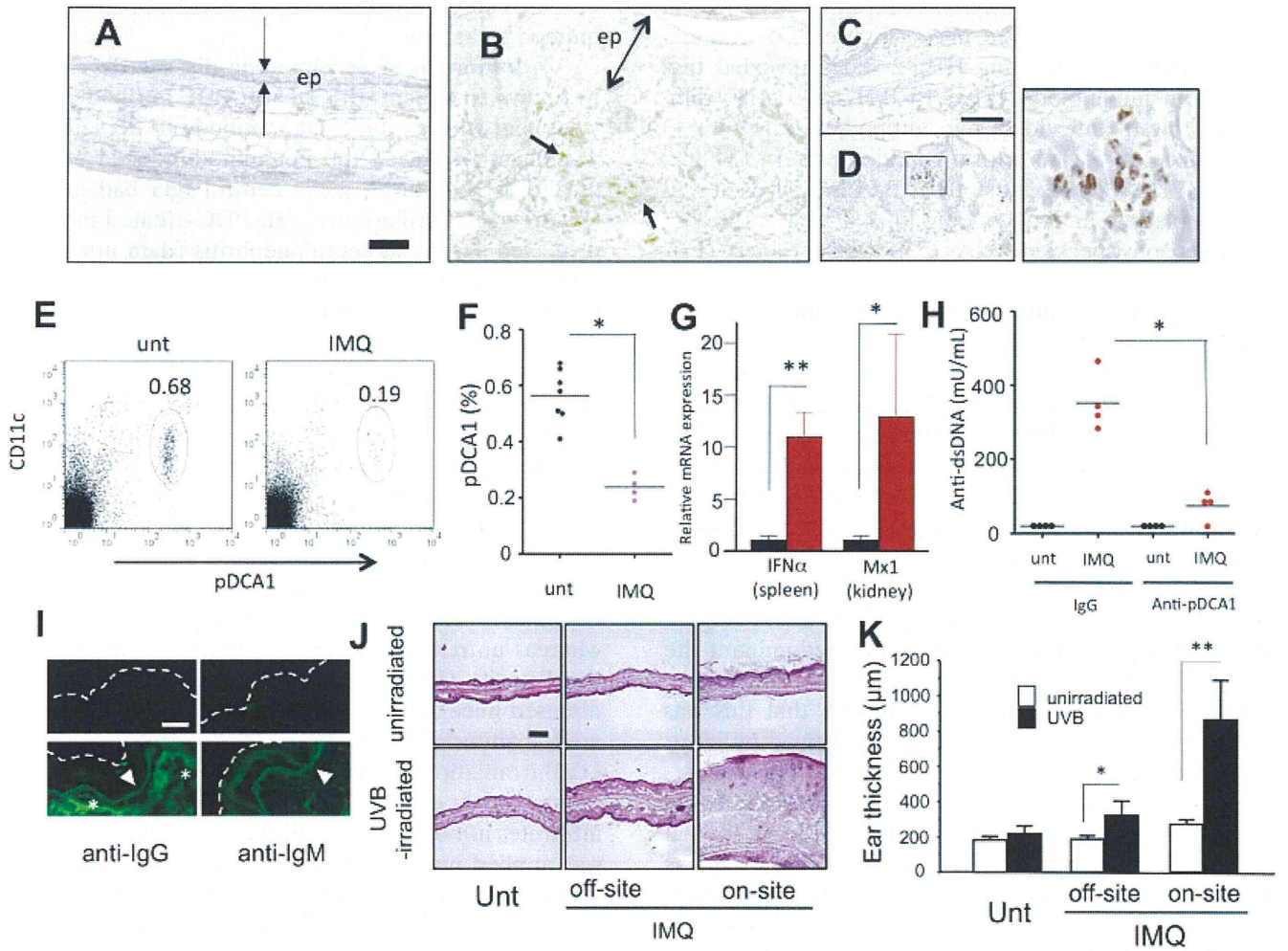

Figure 4. Role of plasmacytoid dendritic cells (PDCs) in autoimmunity induced by topical treatment with imiquimod (IMQ) and skin involvement. **A** and **B**, Staining for anti–plasmacytoid dendritic cell antigen 1 (anti–PDCA-1) in the ear skin of BALB/c mice that were untreated (unt) (**A**) or treated with imiquimod for 1 week (**B**), showing PDC infiltrates in the dermis of the treated mouse (**arrows** in **B**). Epidermis (**ep**) is indicated by the **arrows** in **A** and the **2-headed arrows** in **B**. Bar = 50 μm. **C** and **D,** Immunohistochemical staining for Siglec H, showing no PDCs in the ear skin of untreated control mice (**C**) and an accumulation of PDCs at the epidermal–dermal junction in imiquimod-treated mice. Right, Higher magnification view of the boxed area in **D**. Bar = 100 μm. **E** and **F**, Numbers of PDCs in skin-draining lymph node cells from BALB/c mice that were untreated or treated with imiquimod for 2 weeks, as determined by flow cytometric analysis. * = $P < 0.05$ by Mann-Whitney U test. **G**, Expression of interferon-α (IFNα) and Mx-1 mRNA in the spleen and kidney, respectively, of BALB/c mice that were untreated (black bars; n = 4) or treated with imiquimod for 4 weeks (red bars; n = 4). Transcript values were normalized against hypoxanthine guanine phosphoribosyltransferase. * = $P < 0.05$; ** = $P < 0.01$ by Student's *t*-test. **H**, Anti–double-stranded DNA (anti-dsDNA) titers in BALB/c mice that were untreated or treated with imiquimod for 4 weeks followed by in vivo treatment with IgG or anti–PDCA-1. * = $P < 0.05$ by Mann-Whitney U test. **I,** IgG and IgM deposits in the dorsal skin of FVB/N mice that were untreated (top) or treated with imiquimod for 10 weeks (bottom). Note the distinct linear deposits of immunoglobulin at the basement membrane zone (**arrowheads**) resembling the "lupus band" and the IgG deposition in fibroblasts (**asterisks**). Broken lines indicate the surface of epidermis. Bar = 10 μm. **J,** Hematoxylin and eosin–stained skin from the ears of untreated mice and the left (off-site) and right (on-site) ears of mice treated with imiquimod. Top, Skin that was not exposed to ultraviolet B (UVB) radiation. Bottom, UVB-irradiated skin. Bar = 200 μm. **K**, Thickness of the ears of untreated mice and the left (off-site) and right (on-site) ears of mice treated with imiquimod and not irradiated or exposed to UVB radiation. * = $P < 0.05$; ** = $P < 0.01$ by Student's *t*-test. In **F** and **H**, symbols represent individual mice; horizontal lines show the mean. Values in **G** and **K** are the mean ± SD. Color figure can be viewed in the online issue, which is available at http://onlinelibrary.wiley.com/doi/10.1002/art.38298/abstract.

(24,25). Therefore, repetitive TLR-7 activation in the skin might promote pathogenic B cell activation leading to a class-switch recombination of the γ2a locus. Furthermore, sera from imiquimod-treated mice showed anti-dsDNA, the concentration of which increased over time (Figure 3C). The expression of anti-Sm autoanti-

body, an anti-RNP antibody, was also elevated in FVB/N mice but not in BALB/c mice (Figure 3D). Indirect immunofluorescence using HEp-2 slides revealed that sera from imiquimod-treated FVB/N mice (1:80 dilution) showed anticytoplasmic antibodies only (43.5% penetrance) or ANAs with a speckled pattern (34.8%) (Figure 3E), whereas those from BALB/c mice showed anticytoplasmic antibodies only (44.4% penetrance) or homogeneous/speckled ANAs (55.5% penetrance) (Figure 3F).

Severity of disease caused by intraperitoneal administration of imiquimod. The disease-causing effects of topical and intraperitoneal administration of imiquimod were compared. Compared with topical treatment, intraperitoneal administration resulted in marginal histologic changes in the kidney and liver (data not shown). Correspondingly, the ANA titers in the sera of mice treated intraperitoneally (1:40) were much lower than those in the sera of mice treated topically (1:160). In addition, anti-dsDNA concentrations were not increased by intraperitoneal imiquimod treatment (Figure 3G). This suggests that the skin is the predominant site where TLR-7 agonists initiate lupus-like systemic autoimmune disease. However, it is possible that this was attributable to a lower dose of drug received by intraperitoneal administration.

Accumulation of PDCs in skin and decreased number of PDCs in lymph nodes following topical imiquimod treatment. PDCs constitutively express TLR-7 and TLR-9 and play critical roles in the pathogenesis of SLE through the production of IFNα following TLR-7/TLR-9 activation (5,26). Immunohistochemical analysis using anti–PDCA-1 demonstrated a focal accumulation of PDCs in the dermis of ear skin where imiquimod was applied (Figure 4B), while there were no PDCs in untreated skin (Figure 4A). Staining for Siglec H, a more specific marker for PDCs, confirmed their accumulation at the epidermal–dermal junction (Figures 4C and D). As previously described (27), imiquimod-treated skin showed psoriasis-like changes such as epidermal hyperplasia (Figures 4B and D). In contrast, the numbers of PDCs in skin-draining lymph nodes were significantly decreased following imiquimod treatment (Figures 4E and F). This observation suggested a redistribution of PDCs from lymphoid tissue to the skin where the TLR-7 agonist was applied. This result is similar to the finding that in patients with SLE, the number of circulating PDCs is decreased due to migration to the skin (28,29). A significant increase in *Ifna* expression was observed in the spleen, and increased expression of *Mx1*, the IFNα-stimulated gene (30), was observed in the kidney (Figure 4G), suggesting the role of PDCs in the systemic involvement induced by imiquimod treatment.

Inhibition of autoimmune disease development by in vivo treatment with an anti-PDC antibody. In vivo treatment with an anti-PDC antibody to deplete PDCs significantly reduced the imiquimod-induced elevation of anti-dsDNA titers, while control IgG had no effect (Figure 4H). Furthermore, anti-PDC–treated mice were protected against glomerulonephritis (data not shown). These results strongly suggested that PDCs are essential for the development of the systemic autoimmunity induced by topical imiquimod treatment.

Cutaneous manifestations of murine lupus similar to those of human SLE. Because imiquimod was applied onto the ear skin, the dorsal skin was not inflamed (data not shown). However, the dorsal skin of diseased mice showed linear deposits of IgG and IgM autoantibodies along the basement membrane at the epidermal–dermal junction (Figure 4I) resembling the "lupus band," which is characteristic of SLE. Dermal fibroblasts also showed immunoglobulin deposits, whereas untreated skin was negative for immunoglobulin deposits (Figure 4I). We next examined whether diseased mice showed photosensitivity, which is a common manifestation of SLE. Twenty-four hours after UVB irradiation, imiquimod-treated mice showed acute inflammatory changes such as edema and dermal cell infiltrates not only in the right ear skin where imiquimod was applied but also in the left ear skin, whereas such inflammatory changes were not observed in untreated mice (Figures 4J and K). Thus, the cutaneous manifestations in this lupus model, such as lupus band and photosensitivity, are similar to the cutaneous manifestations of human SLE.

Development of severe autoimmune disease in WT mice following topical treatment with R848. Topical treatment with the TLR-7 agonist R848 also led to autoimmune disease that was similar to or even more severe than that caused by imiquimod and included marked splenomegaly (Figures 5A and B), serum anticytoplasmic autoantibodies and ANAs with a homogeneous pattern (100% penetrance), and high titers of anti-dsDNA (Figures 5C and D). The mice developed severe glomerulonephritis along with tubulointerstitial inflammation (Figures 5E–G). They also showed inflammation in the heart, including pericardial calcification (Figure 5H), which was reminiscent of pericarditis in patients with SLE (31), and myocarditis, as indicated by Mx-1 expression (Figure 5I). In addition, histologic evaluation of the liver revealed severe mononuclear cell infiltration around the portal veins and hepatocyte necrosis (Figure 5J).

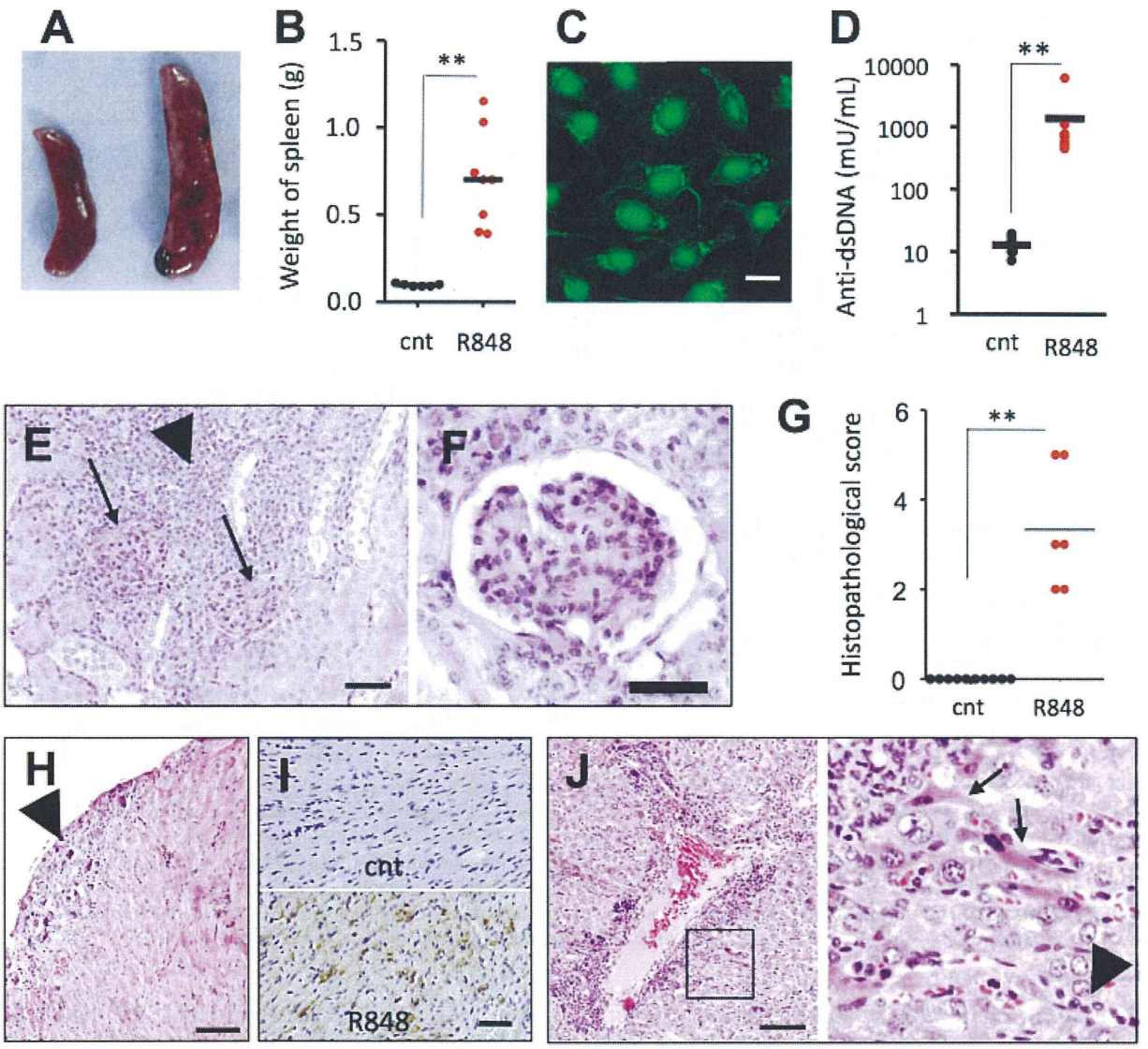

Figure 5. Induction of severe autoimmune disease in BALB/c mice by epicutaneous application of R848. **A** and **B**, Splenomegaly (**A**) and increased spleen weight (**B**) in mice treated with R848 for 8 weeks compared with acetone-treated control (cnt) mice. **C** and **D**, Serum antinuclear antibodies with a homogeneous pattern in HEp-2 cells (**C**) and anti–double-stranded DNA (anti-dsDNA) titers (**D**) in mice treated with topical R848 for 8 weeks. **E**, Periodic acid–Schiff (PAS)–stained histologic sections obtained from mouse treated with R848. Note the cell infiltrates in glomeruli (**arrows**) and intense tubulointerstitial inflammation (**arrowhead**). Bar = 50 μm. **F,** Higher magnification view of section in **E**, showing glomerulonephritis. Bar = 20 μm. **G,** Histopathologic scores in untreated mice and mice treated with R848. **H,** Pericardial calcification (**arrowhead**) in mouse treated with R848 for 4 weeks. Hematoxylin and eosin (H&E) stained. Bar = 100 μm. **I**, Mx-1 expression in the myocardium of control mouse and mouse treated with R848 for 8 weeks. Stained with anti–Mx-1 antibody and counterstained with hematoxylin. Bar = 50 μm. **J**, Histologic evaluation of the liver of mouse treated with R848 for 8 weeks, showing intense inflammatory cell infiltration around the portal veins. The right panel shows a higher magnification view of the boxed area in the left panel. Note the mononuclear cell infiltrates (**arrowhead**) and hepatic necrosis (**arrows**). H&E stained. Bar = 100 μm. In **B**, **D**, and **G**, symbols represent individual mice; horizontal lines show the mean. ** = $P < 0.01$ by Mann-Whitney U test. Color figure can be viewed in the online issue, which is available at http://onlinelibrary.wiley.com/doi/10.1002/art.38298/abstract.

Protection against topical imiquimod–induced autoimmunity in TLR-7–deficient but not TLR-9–deficient mice. TLR-7–knockout mice were used to confirm whether TLR-7 contributes to imiquimod-induced systemic autoimmunity. Although topical imiquimod treatment for 8 weeks profoundly facilitated the expansion of splenic B cells in both WT and TLR-9–knockout mice, this was not the case with TLR-7–

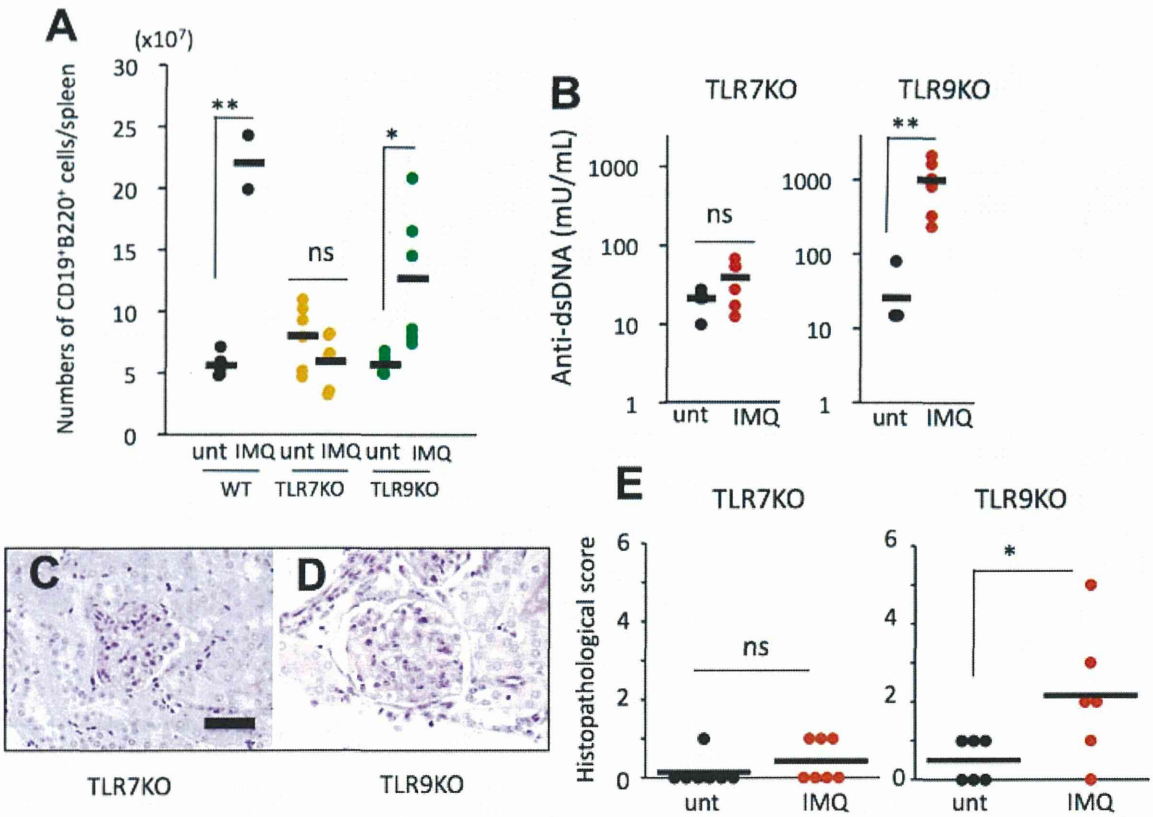

Figure 6. Amelioration of imiquimod (IMQ)–induced autoimmune disease by the Toll-like receptor 7 (TLR-7)–null mutation. **A**, Numbers of splenic B cells in wild-type (WT) mice, TLR-7–knockout (TLR-7–KO) mice, and TLR-9–knockout mice that were untreated (unt) or treated with imiquimod. **B**, Anti–double-stranded DNA (anti-dsDNA) concentrations in TLR-7–knockout and TLR-9–knockout mice that were untreated or treated with imiquimod. **C** and **D**, Representative periodic acid–Schiff–stained kidney sections from TLR-7–knockout (**C**) and TLR-9–knockout (**D**) mice. Bar = 40 μm. **E**, Histopathologic scores in TLR-7–knockout and TLR-9–knockout mice that were untreated or treated with imiquimod. In **A**, **B**, and **E**, symbols represent individual mice; horizontal lines show the mean. * = $P < 0.05$; ** = $P < 0.01$ by Mann-Whitney U test. NS = not significant. Color figure can be viewed in the online issue, which is available at http://onlinelibrary.wiley.com/doi/10.1002/art.38298/abstract.

knockout mice (Figure 6A). In addition, treatment with topical imiquimod did not increase the titers of anti-dsDNA antibodies in TLR-7–knockout mice, while the anti-dsDNA titers in TLR-9–knockout mice (Figure 6B) were as high as those in WT mice (Figure 3C). Correspondingly, TLR-7–knockout mice were protected against the development of glomerulonephritis (Figures 6C and E), which was observed in TLR-9–knockout mice (Figures 6D and E) as in WT mice (Figures 2D and E). Taken together, these results clearly indicate that TLR-7, but not TLR-9, is required for the development of imiquimod-induced systemic autoimmune disease.

DISCUSSION

This study is the first to demonstrate that TLR-7 activation through topical TLR-7 agonist treatment in WT mice leads to lupus-like systemic autoimmune disease. Furthermore, TLR-7 deficiency ameliorates the phenotype, indicating that TLR-7 signaling is necessary for the development of autoimmune disease. Although a prevalence of females is characteristic of human SLE, the effects of topical treatment with TLR-7 agonists, including mortality and morbidity (e.g., kidney disease and autoantibody production) were equal in male and female mice (data not shown). Both serum creatinine levels and proteinuria were increased in imiquimod-treated mice. Therefore, it is likely that renal failure was the cause of death. However, the involvement of multiple organs (including the liver and hematopoietic system) was observed in imiquimod-treated mice; thus, we cannot exclude the possibility that multiplex morbidities led to their death.

The role of TLR-7 in the pathogenesis of SLE has been suggested by several studies using lupus-prone

mice. Male BXSB mice develop lupus because of the *Yaa* locus, which confers a duplication of *Tlr7* (9). In contrast, *Tlr7* deficiency in lupus-prone MRL/*lpr* mice reduced B cell activation and ameliorated renal disease (17). A reduction of the TLR-7 gene dose abolished the *Yaa* phenotype, but increasing the dose promoted fatal acute inflammatory pathology (16). Thus, it is likely that homeostatic TLR-7 activation by repetitive treatment of WT mice with topical imiquimod or R848 leads to autoimmune disease, which might be analogous to increasing the TLR-7 gene dose.

It has been suggested that TLR-7 and TLR-9 might have opposing contributions to autoimmune pathology (17,32). A recent study demonstrated that TLR-9 protected against autoimmune disease by antagonizing TLR-7 (18). More recently, a role of UNC93B1, an endoplasmic reticulum–resident protein, was shown to control the intracellular trafficking of TLR-9 and TLR-7 (33). TLR-9 competes with TLR-7 for UNC93B1-dependent trafficking and predominates over TLR-7, thereby regulating homeostatic TLR-7 activation. Reciprocal TLR-7/TLR-9 balance, which is dependent on UNC93B1, is required for limiting systemic autoimmunity (34). However, in our experimental setting, TLR-9–knockout mice did not show an increased response to imiquimod compared with WT mice with respect to disease induction.

PDCs play a critical role in the pathogenesis of SLE through IFNα production upon TLR-7/TLR-9 ligation (5,35). IFNα released from PDCs promotes autoreactive B cell expansion, causes the differentiation of plasma cells to produce autoantibodies, and activates myeloid cells and autoreactive T cells (3,35). The essential role of PDCs in the development of autoimmune disease was clearly demonstrated by depleting them. Anti–PDCA-1, used for the depletion of PDCs, recognizes the bone marrow stromal cell marker antigen 2, which is expressed predominantly by PDCs but also by other myeloid cells following stimulation with IFNs (36). Therefore, in vivo treatment with anti–PDCA-1 might affect some population(s) of myeloid cells as well. The targeted depletion of Siglec HG–expressing cells (37), for example, will help further clarify the role of PDCs in imiquimod-induced lupus in the future.

We demonstrate here that compared with intraperitoneal administration of imiquimod, topical application of imiquimod to the skin efficiently promotes systemic autoimmune disease, although it was not determined how much imiquimod was substantially absorbed from the skin. Topical treatment with R848 also induces severe systemic autoimmune disease, including nephritis and hepatitis, whereas internal organ involvement was not observed in mice when R848 was administered intraperitoneally (38). Furthermore, a recent study in which inflammatory responses in rats treated with subcutaneous and intraperitoneal imiquimod were compared clearly indicated that more potent systemic effects were elicited by subcutaneous injection (39). Therefore, subsequent systemic effects of TLR-7 triggering might be largely dependent on the treatment site. Imiquimod has been used to treat various skin neoplasms, including genital warts, actinic keratoses, and superficial basal carcinomas (40). As far as we know from the literature, however, there has been no case in which the development of SLE resulted from imiquimod treatment. We have had some patients with actinic keratoses in whom transient ANA positivity developed during treatment with imiquimod, but SLE did not develop afterward. This suggests that therapeutic doses of imiquimod are relatively smaller than those that induce autoimmune disease in mice. In fact, the dose of imiquimod used for mice in this study (41.7 mg/kg) was 200-fold higher than the clinical dose used in humans (0.21 mg/kg).

Topical imiquimod treatment induced psoriasis-like epidermal hyperplasia and inflammatory cell infiltrates, as previously demonstrated (41). PDC accumulation was observed in the dermis of imiquimod-treated mice, similar to human psoriasis (42). Furthermore, topical application of imiquimod aggravated psoriatic lesions through PDC activation, suggesting the role of TLR-7–mediated innate immunity in the pathogenesis of psoriasis (27). In our experimental setting, however, full-blown psoriatic lesions were observed within 3 weeks of imiquimod treatment but were attenuated thereafter (data not shown). Likewise, a previous study demonstrated imiquimod-induced skin lesions within 1 week of imiquimod treatment (41). Similar to psoriasis, cutaneous lesions of lupus are frequently associated with PDC infiltrates (43,44). Furthermore, topical application of imiquimod led to a histopathologic pattern similar to that of cutaneous lupus in humans (45). Thus, it is likely that the pathogenesis of both psoriasis and lupus share roles of PDCs and type I IFN.

Potential candidates for naturally occurring TLR-7 ligands are RNA viruses such as endogenous retrovirus, because "pseudoviral" immunity is evolving as a recent concept in understanding the pathogenesis of SLE (13,46). UV radiation is a worsening factor not only for cutaneous lesions but also for systemic symptoms in patients with SLE. It was previously shown that UV light–induced injury led to an amplification cycle of cutaneous lupus through activation of autoimmune T